




Numerical Modeling of Compartment Fires: Ventilation Characteristics and Limitation of Kawagoe's Law

Zilong Wang, Tianhang Zhang and Xinyan Huang ^{*}, Research Centre for Fire Safety Engineering, Department of Building Services Engineering, The Hong Kong Polytechnic University, ZS 832, BLK Z, 181 Chatham Road South, Hung Hom, Kowloon, Hong Kong

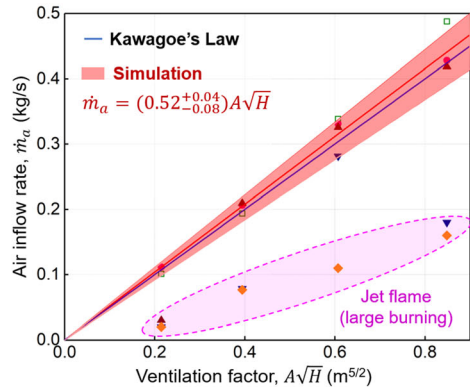
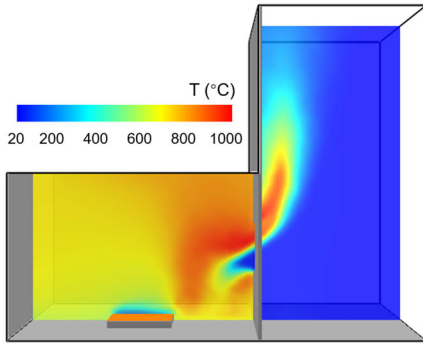
Received: 3 August 2021/**Accepted:** 3 February 2022/**Published online:** 9 March 2022

Abstract. Kawagoe's Law is an essential correlation in compartment fire research, which defines the relationship between the ventilation factor and maximum fuel burning of the compartment. Although this law has been widely used, there is still a lack of numerical validation and knowledge on the limiting conditions of its application. In this paper, a numerical study is conducted under full-scale compartment fire with different opening sizes and gas fuel supply rates using the LES model for validating Kawagoe's Law. The mass flow rate of inflow through the opening and the indoor heat release rate is focused during the numerical validation. Numerical results show that the inflow rate and indoor heat release rate comply well with Kawagoe's Law under ordinary openings with a small aspect ratio. However, Kawagoe's Law becomes less valid for openings with large aspect ratios and small-gap openings. The jet flame was observed in the case of openings with large aspect ratios under a high fuel supply rate. For compartment fires with small gaps, a breathing process, i.e., the periodical suppression and revitalization of the fire, is modeled. This work provides practical guidance for modeling compartment fires and paving the way for constructing a numerical compartment fire database.

*Correspondence should be addressed to: Xinyan Huang, E-mail: xy.huang@polyu.edu.hk



Graphical Abstract



Keywords: Fire simulation, Enclosure fire, Small opening, Flashover limit, Jet flame, Heat release rate

Abbreviations

CFD	Computational fluid dynamics
FDS	Fire dynamics simulator
HRR	Heat release rate
HRRPUV	Heat release rate per unit volume

List of Symbols

A	Area of the opening (m ²)
c_p	Specific heat (kJ/(kg K))
C	Fitting coefficient (-)
D^*	Characteristic diameter
g	Acceleration of gravity (m/s ²)
H	Height of the opening (m)
\dot{m}	Mass flow rate (kg/s)
\dot{Q}	Heat release rate of fire (kW)
T	Temperature (K)
W	Width of the opening (m)

Greek Letters

ρ	Density (kg m ⁻³)
δ_x	Nominal grid size

Superscripts

K	Kawagoe's Law
---	---------------

Subscripts

a	Air
F	Fuel

g	Gas
in	Inside the compartment
jet	Jet flame
∞	Ambient

1. Introduction

The compartment fire or enclosure fire is one of the most common building fire scenarios that cause enormous casualties (Figure 1), because of the trapped toxic smoke and enhanced heating inside a confined space [1]. The compartment fire can also develop into a flashover and generate spilled flame that can initiate a facade fire, such as the tragic Grenfell Tower fire [2]. Despite the simple configuration and fire scenario, it is still challenging to predict the compartment-fire development and its influence on the building structure and people due to the complex heat transfer and combustion processes [3]. In fact, it took many decades of research to form a scientific understanding of the compartment fire [4]. Before the 1950s, it was believed that the intensity and hazard of a compartment fire were controlled by the amount of fuel, and different stages of compartment fire were not clearly identified. Thus, typical fire size and fire load densities were assumed for various occupancies in the fire engineering design.

In the late 1950s, Kawagoe (1958) summarized his decade’s work on compartment fires since 1948 and revealed the correlation for the mass inflow rate and fuel-burning rate during the fully-developed (post-flashover) fire stage by assuming stoichiometric combustion of wood and uniform compartment temperature and using the Bernoulli equation and mass conservation. The famous Kawagoe’s Law for the fully developed compartment fire was then proposed and verified by the test data of fuel burning rate. That is, the mass-loss or burning rate (\dot{m}_F^K) of wood and inflow rate (\dot{m}_a^K) are correlated to the characteristics of the openings, as further summarized in [6]

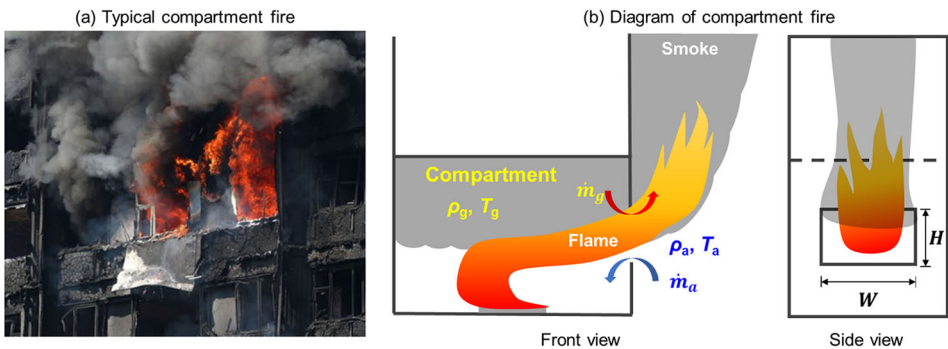


Figure 1. a Typical compartment fire observed in the 2017 Grenfell Tower fire, and b a schematic diagram of the compartment fire with one opening.

$$\dot{m}_F^K = C_F AH^{1/2} = 0.09 AH^{1/2} (kg/s) \quad (1)$$

$$\dot{m}_a^K = C_a AH^{1/2} = 0.5 AH^{1/2} (kg/s) \quad (2)$$

which indicates that the fully developed compartment fire is controlled by the ventilation factor ($AH^{1/2} = WH^{3/2}$), rather than the fuel load. These correlations were validated by different scales of experiments with compartment volumes ranging from 0.032 m³ to 125 m³ [5] and multiple openings, and their relative uncertainty is about 30% (see details in the [Appendix](#)). Today, the concepts of over- and under-ventilated fires have been widely used to describe pre- and post-flashover compartment fires.

Note the burning rate coefficient ($C_F = 5.5$) in Eq. (1) was measured and valid only for the wood fuel in Kawagoe's original experiments, which changes with the fuel type. Thus, Kawagoe's Law correlating the inlet airflow in the form of Eq. (2) is more widely used. Both experiments and theoretical analysis suggest that Kawagoe's Law is most valid in fully developed fires, where the compartment is filled with hot gases and smoke above 800 K.

By assuming the constant heat of oxidation (13.1 MJ/kg) [7] for most common fuels and the complete consumption of inlet oxygen (i.e., the principle of oxygen calorimetry), the Kawagoe's Law can further predict the maximum fire heat release rate (HRR) or fire power inside the compartment as [8, 9]

$$\dot{Q}_{in}^K = 1500 AH^{1/2} (kW) \quad (3)$$

Kawagoe's Law in the forms of Eqs. (1–3) not only lays a solid foundation for the modern research of compartment fire, spill plume, and facade fire [10] but also helps establish the structure fire resistance tests. Over the last few decades, Kawagoe's Law has been verified and corrected in many fire tests and theoretical derivations by other researchers. The tests found the burning-rate fitting coefficient (C_F) of 5.5 in Eq. (1) varied from 5.0 [11] to 6.0 [12–14], and the inflow fitting coefficient (C_a) of 0.5 in Eq. (2) varied from 0.40 to 0.61 [15], all of which are within the uncertainty of Kawagoe's fire tests.

For the original Kawagoe's Law, it is assumed that the mass inflow rate is equal to the mass outflow rate in the compartment fire and the mass produced inside the compartment is ignored. When the generation of fuel gas inside the compartment is considered, more theoretical derivation gives the correction of Eq. (2), such as [1, 16],

$$\dot{m}_a = \frac{2.1 AH^{1/2}}{(1.6(1 + \dot{m}_F/\dot{m}_a)^{2/3} + 1)^{3/2}} (kg/s) \quad (4)$$

$$\dot{m}_a = 0.5 AH^{1/2} - 0.53 \dot{m}_F (kg/s) \quad (5)$$

According to Eqs. (1–5), the validity of using the ventilation factor has been confirmed theoretically. Thus, the concepts of ventilation factor and ventilation-controlled fire have been adopted globally in both the fire safety design and firefighting [17].

Because it is difficult to measure the exact inlet airflow profiles in compartment fire tests, the airflow rate in most studies could only be estimated from the fuel mass loss rate [18]. Other researchers [15, 19, 20] used the temperature profile to assess the inlet air flow rate, which showed reasonable consistency with Eq. (2). In terms of the maximum HRR inside the compartment, Lee et al. (2007) manually controlled the mass flow rate of the fuel to an enclosure of 0.125 m^3 and found that the HRR, measured by oxygen calorimetry, agreed well with Eq. (3).

Driven by the rapid development of computational fluid dynamics (CFD), the CFD-based numerical simulations have been applied in compartment fire modeling [21]. For simulating over-ventilated (or pre-flashover) compartment fires, Chow et al. (2005; 2012) found that the inlet airflow was also proportional to the ventilation factor ($AH^{1/2}$), agreeing with the theoretical analysis [1, 5]. For simulating under-ventilated (or fully-developed) compartment fires in a $0.5 \text{ m} \times 0.5 \text{ m} \times 0.5 \text{ m}$ chamber, Zhao et al. (2016) showed that both the inflow rate ($0.41 \text{ kg}AH^{1/2}/\text{s}$) and the HRR ($1131 \text{ kW}AH^{1/2}$) inside the compartment were 20% lower than Kawagoe's Law in Eq. (3). Afflard et al. (2019) simulated the HRR ($925 \text{ kW}AH^{1/2}$) inside a 1/4 scale ISO9705 enclosure ($0.6 \text{ m} \times 0.9 \text{ m} \times 0.6 \text{ m}$), which was beyond the uncertainty limit of Kawagoe's Law. To the best of the authors' knowledge, there is no numerical simulation of real-scale compartments that systematically verifies the Kawagoe's Law and identify its limiting conditions. Without these basic validations, it is challenging to further simulate more complex compartment fires, spilled flame, and facade fires.

To fulfil this knowledge gap, this work performs a numerical study of a full-scale compartment fire (ISO 9705: $3.6 \text{ m} \times 2.4 \text{ m} \times 2.4 \text{ m}$) to use numerical fire simulation to validate Kawagoe's Law. Then, the special opening conditions (i.e., the opening with large aspect ratios and small gaps) are modeled to explore the limiting conditions of applying Kawagoe's Law.

2. Numerical Modeling

2.1. Compartment Model

In this study, a full-scale ISO 9705 compartment (Figure 2) was built in FDS 6.7.5 [26]. The dimension of the compartment is 3.6 m (*length*) \times 2.4 m (*width*) \times 2.4 m (*height*). In connection with the compartment, an external open space with dimensions of 2.4 m (*length*) \times 2.4 m (*width*) \times 4.8 m (*height*) is also modeled. All walls are set as the external boundary of the computation domain allows the heat transfer from the compartment to the ambient. The front wall has a thickness of several computational cells to provide the required space for the airflow through the opening [27]. All walls, including the facade wall consist of one ceramic fiber layer with the thickness of 2.5 cm and one gypsum layer with the thickness of 1.2 cm.

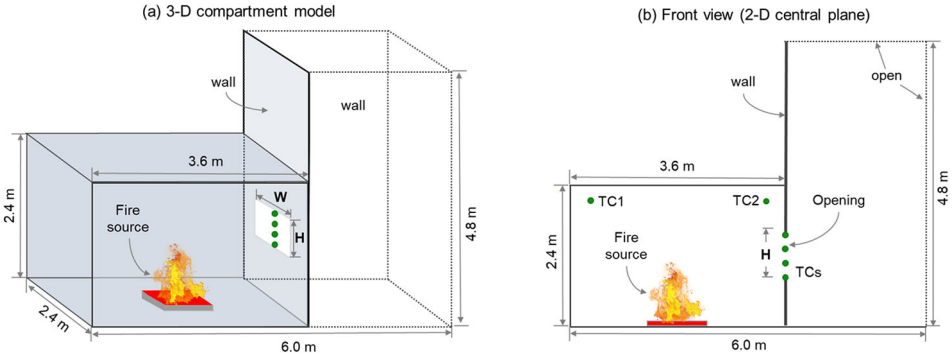


Figure 2. Illustration of the numerical model for compartment fire, a 3-D model, and b side view or the simplified 2-D model.

The detailed description of the experimental setup and thermal properties of walls and the floor are recommended by NIST [28, 29]. The detailed validation of multiple compartment fire experiments [29] shows that FDS can well simulate the full-scale compartment fires.

One window opening was modeled as a rectangular hole in the center of the front wall with an adjustable size. Parameters to be measured in the model mainly include (1) the opening flow characteristics using 2-D planar devices (normal to the opening), (2) the HRR inside the compartment using the volumetric device, and (3) slices of temperatures, flow velocity, oxygen concentration, and heat release rate per unit volume (HRRPUV) at the central plane (see the front view in Figure 2b). Besides, temperature sensors, located 10 cm below the ceiling of the compartment (TC1 and TC2) and vertically distributed at the centerline of the opening are used to determine the development of the fire. The simulation time was set as 1200 s for each compartment fire scenario, which is sufficient for these parameters to reach the steady state.

2.2. Simulation Setup

For the original 3-D compartment model (Figure 2a), both the height and the width of the opening are varied. In total, four different opening sizes are considered in the model, $0.4 \text{ m} \times 0.6 \text{ m}$, $0.6 \text{ m} \times 0.8 \text{ m}$, $0.8 \text{ m} \times 0.8 \text{ m}$, and $0.8 \text{ m} \times 1.0 \text{ m}$, and their ventilation factor ranges from 0.19 to $0.8 \text{ m}^{5/2}$, as summarized in Table 1. The default Large Eddy Simulation (LES) turbulence model was employed, and a single-step and mixing-controlled combustion model was adopted. To simulate the flame extinction inside the compartment, an extinction model based on critical flame temperature is adopted to determine whether combustion can continue. If the oxygen and fuel are not sufficient to raise the grid temperature to the critical flame temperature, the combustion is regarded as not viable. In this model, a critical flame temperature of $1507 \text{ }^\circ\text{C}$ is used with a methane burner to model the suppression of the compartment fire.

A methane burner with the SOOT_YIELD of 0.001 is placed in the center of the compartment as the fire source, where the heat of combustion for methane (CH₄) is 52.4 MJ/kg. Giving the stoichiometric methane/air ratio of 0.058 kg/kg, Kawagoe's Law predicts that the required burning rate of methane (\dot{m}_F^K) for the fully-developed compartment fire is controlled by the incoming airflow (or ventilation controlled) as

$$\dot{m}_F^K(\text{CH}_4) = 0.058\dot{m}_a^K = 0.058 \times 0.5AH^{1/2} = 0.029AH^{1/2}(\text{kg/s}) \quad (6)$$

which will be used as a reference value throughout the following validation. Note that the burning rate coefficients ($C_F = 0.029$) is for methane, which is different from Kawagoe's original expression ($C_F = 0.09$ in Eq. 1) for burning wood cribs. A predefined constant fuel burning rate (\dot{m}_F) is varied from $0.4\dot{m}_F^K$ to $3.5\dot{m}_F^K$ for simulating different fire scenarios. All simulation cases are listed in Table 1.

In addition, for the compartment with a wide opening, i.e., a large aspect ratio (W/H), or a gap below eaves, the 3-D model may be simplified into a 2-D model (Figure 2b), which can significantly save the computational time. Nevertheless, the accuracy of such a simplified 2-D compartment fire has not been fully explored, so it is unclear whether it can also validate Kawagoe's Law, so that 2-D simulations are also performed to see the impact of model simplification. In the 2-D compartment model, the width of the opening is set the same as 2.4 m, and the opening height changes from 0.06 m to 0.5 m to vary the ventilation factor. The smaller gap heights from 0.06 m to 0.1 m are adopted to explore common compartment fires with a limited oxygen supply, where the air only flows through the gaps of the door and eaves. Thus, the aspect ratio (W/H) modeled in this work varies in a wide range from 0.67 to 40 (small gap), as summarized in Table 1.

2.3. Grid Sensitivity Study

For a field fire model, the grid size is one of the important parameters that affect the accuracy of the simulation results [30, 31]. Thus, two criteria were adopted to choose the cost-effective grid size, including the fire diameter and opening criterion. For a buoyancy-controlled fire, a non-dimensional value D^*/δ_x was employed to judge the fitness of the grid size. The characteristic diameter D^* is given as

$$D^* = \left(\frac{\dot{Q}}{\rho_\infty c_p T_\infty \sqrt{g}} \right)^{2/5} \quad (7)$$

where δ_x is the nominal grid size. The value of D^*/δ_x can be regarded as the number of computational cells, where the characteristic diameter of fire is divided. In general, the more cells the characteristic diameter of the fire is divided into, the higher is the accuracy of the model computation. According to McGrattan's suggestion [32], D^*/δ_x should be larger than 10 to achieve accurate simulation results. Besides, since the near-field reacting (combustion) region, e.g., the opening region

Table 2
Maximum Grid Sizes for Small Fire HRRs, where finer cells are used at the level of opening

W (m)	H (m)	\dot{m}_F (kg/s)	\dot{Q}_F (kW)	D^*	$(A\sqrt{H})^{2/5}$	$\frac{2WH}{(W+H)}$	Cell size combination
0.4	0.6	0.0022	113	0.40	0.51	0.48	0.04 m + 0.02 m
0.6	0.8	0.0050	262	0.56	0.71	0.69	0.05 m + 0.025 m
0.8	0.8	0.0067	349	0.63	0.80	0.80	0.05 m + 0.025 m
0.8	1.0	0.0093	488	0.72	0.91	0.89	0.05 m + 0.025 m
2.4	0.06	0.00040	21	0.21	0.26	0.12	0.02 m + 0.01 m
2.4	0.08	0.00060	33	0.25	0.31	0.15	0.02 m + 0.01 m
2.4	0.1	0.00090	46	0.28	0.35	0.19	0.02 m + 0.01 m
2.4	0.2	0.0025	131	0.43	0.54	0.37	0.02 m + 0.01 m
2.4	0.3	0.0046	241	0.54	0.69	0.53	0.05 m + 0.025 m
2.4	0.4	0.0071	371	0.64	0.82	0.69	0.05 m + 0.025 m
2.4	0.5	0.0099	518	0.74	0.94	0.83	0.05 m + 0.025 m

is a region of interest, a stricter fire diameter criterion of $D^*/\delta x \geq 20$ is adopted for the meshes in the vicinity of the opening to ensure accurate simulations.

For the opening, two length scale ratios, $(A\sqrt{H})^{2/5}/\delta_x$ and $2WH/(W+H)/\delta_x$, were proposed by Zhao et al. [24] to meet the demand for solving the vent flow sufficiently well, which should be greater than 10 to achieve an accurate prediction of air flows. Based on these criteria, the maximum grid size for each case under the minimum predefined fuel burning rate ($0.4\dot{m}_F^K$) is summarized in Table 2, and the combined grid settings that satisfy the above criteria are adopted for the compartment fire modeling. In each combination grid, the finer grid was placed at the level of the opening and extended 0.4 m into the compartment and out of the opening, respectively. The larger grid was used in the rest of the computation domain to save computational cost.

A grid sensitivity study was conducted by simulating the compartment fire with an opening of 2.4 m \times 0.5 m ($A\sqrt{H} = 0.85$) under the burning rate of $0.4\dot{m}_F^K$ (i.e., an over-ventilated fire HRR of 500 kW) using different grid resolutions. Four different grid resolutions were considered: (1) 0.1 m and 0.05 m, (2) 0.1 m and 0.025 m, (3) 0.05 m and 0.025 m, and (4) 0.04 m and 0.02 m. For these grid size combination, the finer grid is used near the openings and the coarser grid is adopted used in the rest of the computation domain.

The average temperature and horizontal velocity from 600 to 1200 s at the middle of the opening plane are shown in Figure 3. Based on the grid sensitivity analysis, the temperature and horizontal velocity distribution at the middle of the opening plane when using the combination grid of 0.05 m and 0.025 m (near the opening) are close to the modeling results with a finer grid. Similar results are found in other cases. Thus, the combined grid is sufficient to guarantee the grid independence of computational results.

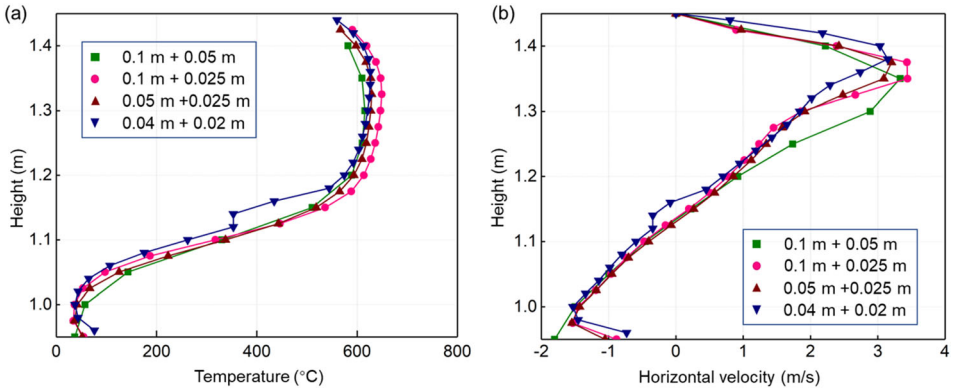


Figure 3. Grid resolution effect on the distribution of a temperature and b horizontal velocity at the middle of the opening ($2.4 \text{ m} \times 0.5 \text{ m}$ and $A\sqrt{H} = 0.85$), where the HRR of the over-ventilated fire is 500 kW .

3. Numerical Results and Discussion

3.1. Validation of Kawagoe's Law for Ordinary Openings

By setting different fuel mass flow rates, both over-ventilated and under-ventilated compartment fires can be observed under different ventilation conditions. The compartment with a $0.6 \text{ m (W)} \times 0.8 \text{ m (H)}$ opening ($A\sqrt{H} = 0.43$) is taken as an example to show the simulation results. The detailed evolution of the HRRPUV that represents the presence of the flame is also compared in Video S1. In general, all compartment fires reach a semi-steady state in a few minutes (see Figure 13), so the averaged parameters including temperature, mass flow rate and HRR between 600 and 1200 s are shown. Figure 4 compares the time-averaged temperature distribution of the compartment fire under predefined fuel generation rates of 0.0075 kg/s ($0.6\dot{m}_F^K$ and 393 kW for an over-ventilated fire), 0.0125 kg/s (\dot{m}_F^K and 655 kW for the flashover limit), and 0.0188 kg/s ($1.5\dot{m}_F^K$ and 985 kW) and 0.0375 kg/s ($3\dot{m}_F^K$ and 1.97 MW) for a under-ventilated fire.

In the case with the fuel generation rate of $0.6\dot{m}_F^K$, The high-temperature area is mainly concentrated near the source of the fire, and there are two zones, a hotter upper zone, and a cooler lower zone, as seen in Figure 4a. Also, all fuel gases are burned out in the compartment, and flames only exist inside the compartment (i.e., no spilled flame, also see Video S1). For the compartment fire with a fuel generation rate of 0.0125 kg/s (\dot{m}_F^K , the same as Kawagoe's prediction and near the flashover limit) in Figure 4b, in addition to the combustion inside the compartment, a small flame is spilled out from the opening to seek more oxygen, indicating that the fire just becomes fully developed or under-ventilated. At this point, the compartment is filled with hot gases that has a uniform temperature of almost $800 \text{ }^\circ\text{C}$.

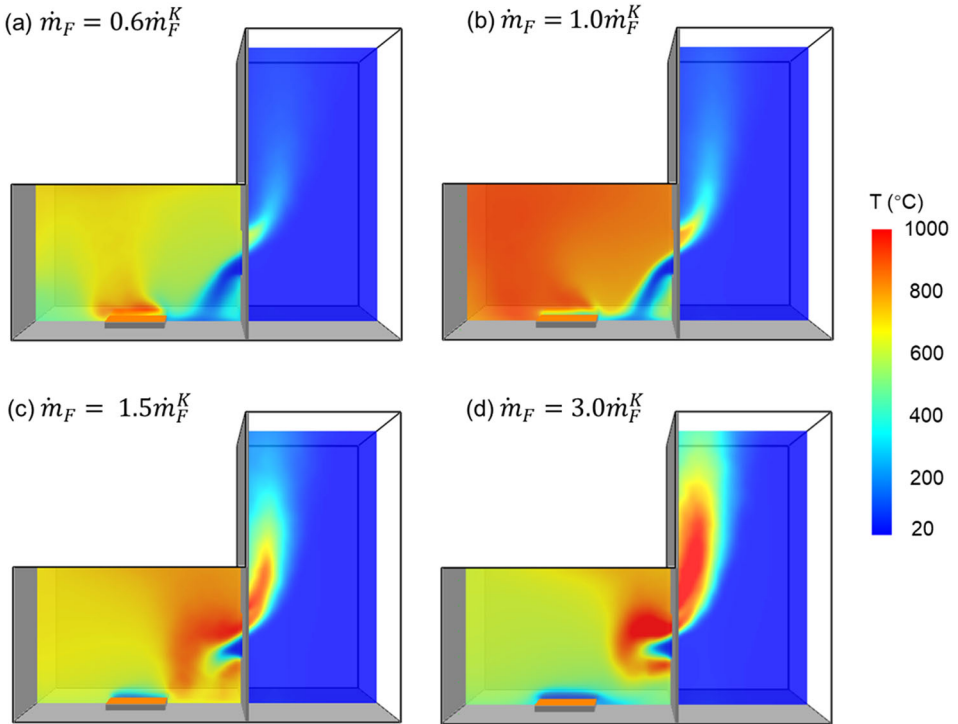


Figure 4. Time-averaged temperature distribution of the compartment fire with a 0.6 m (W) \times 0.8 m (H) opening ($A\sqrt{H} = 0.43$), under fuel generation rates of a 0.0075 kg/s ($0.6\dot{m}_F^K$ and 393 kW for an over ventilated fire), b 0.0125 kg/s (\dot{m}_F^K and 655 kW for the flashover limit), c 0.0188 kg/s ($1.5\dot{m}_F^K$ and 985 kW), and d 0.0375 kg/s ($3\dot{m}_F^K$ and 1.97 MW) for a under-ventilated fire.

With greater fuel generation rates of 0.0188 kg/s ($1.5\dot{m}_F^K$) and 0.0375 kg/s ($3\dot{m}_F^K$) in Figure 4c-d, a larger spilled flame is observed outside the opening, so that more fuels are consumed by oxygen outside the compartment rather than inside. Therefore, the indoor HRR is determined by the ventilation condition instead of the fuel supply. Moreover, the overall temperature inside the compartment actually decreases, and the high-temperature area in the compartment moves from the fire source to the opening. This phenomenon agrees with recent experimental measurements for a reduced-scale (0.4 m cubic) compartment fire [33]. Nevertheless, the high-temperature region still exceeds 600 °C, so that it is still reasonable to use a smoke layer temperature of above 600 °C to judge the occurrence of flashover.

Figure 5 shows the rate of incoming airflow and the indoor HRR under different ventilation factors vs. the normalized fuel generation rate (\dot{m}_F/\dot{m}_F^K). Simulation results confirm that the mass flow rates of inflow (\dot{m}_a) are basically the same under the same ventilation factor in both over-ventilated and under-ventilated sce-

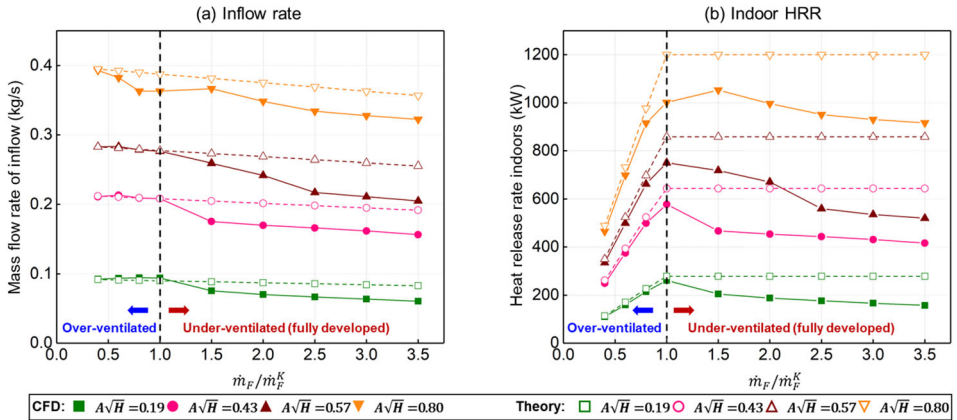


Figure 5. a Rate of incoming airflow, and b the indoor HRR under different ventilation factors vs. the normalized fuel generation rate (\dot{m}_F/\dot{m}_F^K), where the dashed line indicated the flashover limit predicted by the Kawagoe’s law.

narios, with a slight decrease as the fuel supply rate increase. This means that even in over-ventilated scenarios, although the HRR of compartment fires is controlled or limited by the fuel, the mass inflow rate is still determined by the ventilation factor.

Figure 5a also compares the numerical data and the prediction of the inflow rate using the updated Kawagoe’s Law in Eq. (5), which corrected the influence of fuel. In general, a good agreement between numerical and theoretical values in the over-ventilated stage. However, for the under-ventilated or fully developed stage, the numerical inflow rate is 5% to 25% less than the theoretical value from Eq. (5), and the deviation increases as the fuel supply increases. This is because the spilled flame heats the air outside the compartment, which makes the density of preheated incoming air lower. Thus, the actual inflow rate is lower than the theoretical values from Eqs. (2) and (5), and the indoor HRR is reduced. The detailed process of air inflow reduction caused by the spilled flame is shown in Figure 14.

For the indoor HRR (Figure 5b), it increases with the increasing fuel supply in the over-ventilated compartment fire or pre-flashover condition ($\dot{m}_F/\dot{m}_F^K \leq 1$), that is, the fire is fuel controlled. Once the fuel supply exceeds the Kawagoe limit ($\dot{m}_F/\dot{m}_F^K \geq 1$), the indoor HRR continuously decreases, rather than keeping the theoretical value from Eq. (3). There are two reasons, (1) the preheating of inflow reduce the air density and mass flow rate, and (2) the increasing indoor fuel supply with limited oxygen supply cause incomplete combustion [24]. It is expected that as the indoor fuel supply further increases, the inflow rate (\dot{m}_a) and indoor HRR will continue to decrease, and eventually the compartment becomes a gas burner without inflow air and indoor HRR (discussed more in Sect. 3.2).

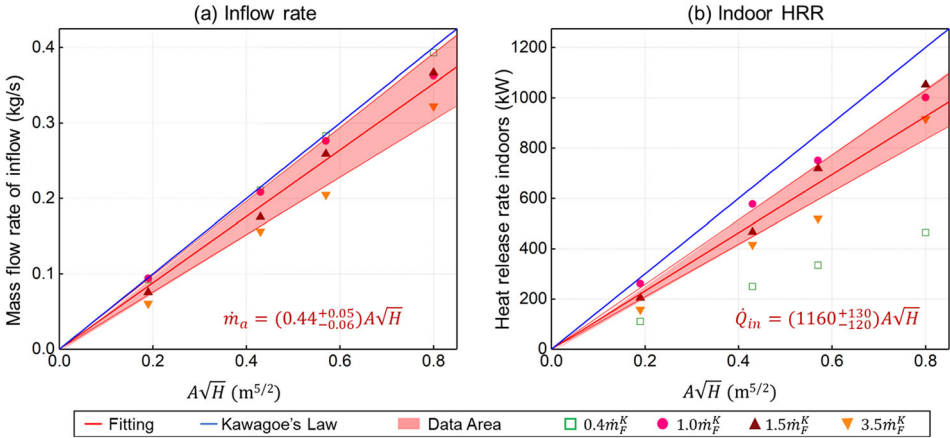


Figure 6. a Mass flow rate of inflow (\dot{m}_a), and b indoor HRR under different fuel supply rates (\dot{m}_F) and ventilation factors ($AH^{1/2}$) in the 3D model.

To further verify Kawagoe’s Law, linear regression is applied to correlate the inflow rate (\dot{m}_a) and indoor HRR with the ventilation factor. The overall correlation as well as the correlation for different fuel supply rates (\dot{m}_F/\dot{m}_F^K) is shown in Figure 6. For the inflow air rate, the numerical result ($\dot{m}_a = 0.44AH^{1/2}$) is quite close to Kawagoe’s Law, and it is also within the range of 0.4–0.61 given by Rockett (1976). The inflow coefficient (C_a) decreases from 0.49 to 0.38, when the fuel supply rates (\dot{m}_F/\dot{m}_F^K) increases from 0.4 (over-ventilated) to 3.5 (under-ventilated).

The relationship between indoor HRRs and ventilation factors is only considered in the under-ventilated stage and post-flashover scenarios. The maximum indoor fire HRR ($\dot{Q}_{in}^{max} = 1290AH^{1/2}$) occurs under the fuel supply of \dot{m}_F^K , while it drops to $\dot{Q}_{in} = 1040AH^{1/2}$, when the fuel supply rate is $3.5\dot{m}_F^K$. The average indoor HRR follows $\dot{Q}_{in} = 1160AH^{1/2}$, which is 23% lower than theoretical value of $1500AH^{1/2}$ in Eq. (3) but still within the uncertainty of Kawagoe’s experiments (see Appendix).

These numerical results show that the mass flow rate of inflow and the indoor HRR increases linearly with the ventilation factor ($AH^{1/2}$) in accordance with the principle of Kawagoe’s Law. The numerical simulations also demonstrate that Kawagoe’s Law gives the theoretical maximums of the inflow rate and the indoor HRR, and the values in actual fire scenarios (both over-ventilated and under-ventilated fires) are lower than these theoretical values. To be noted, even for an over-ventilated pre-flashover compartment fire, the linear correlation with ventilation factor can also be used to estimate the inflow mass flow rate, which follows Bernoulli’s principle. However, the HRR of over-ventilated fire increases with the fuel supply rate, because the fire is fuel controlled rather than ventilation controlled. Therefore, Kawagoe’s Law is an essential correlation in compartment fire

research, and the CFD-based numerical results in this work provide a good validation of Kawagoe's Law.

3.2. Compartment Fires with an Opening of Large Aspect Ratio

For the compartment opening with a large aspect ratio, the 2-D model could be a cost-effective simplification to simulate the compartment fire, because the influence of the width of the opening becomes small in these fire scenarios. The simulation results of the 2-D model were demonstrated under different fuel supply rates in Figure 7 by using a wide compartment opening (2.4 m wide and 0.3 m high) as an example. The fire behaviors of each compartment fire were also displayed in Videos S2. With a ventilation factor and fuel supply similar to the compartment with a 0.6 m by 0.8 m opening, the time-averaged temperature distribution of the compartment fire is similar to 3D modeling results in Figure 4, and the spilled hot

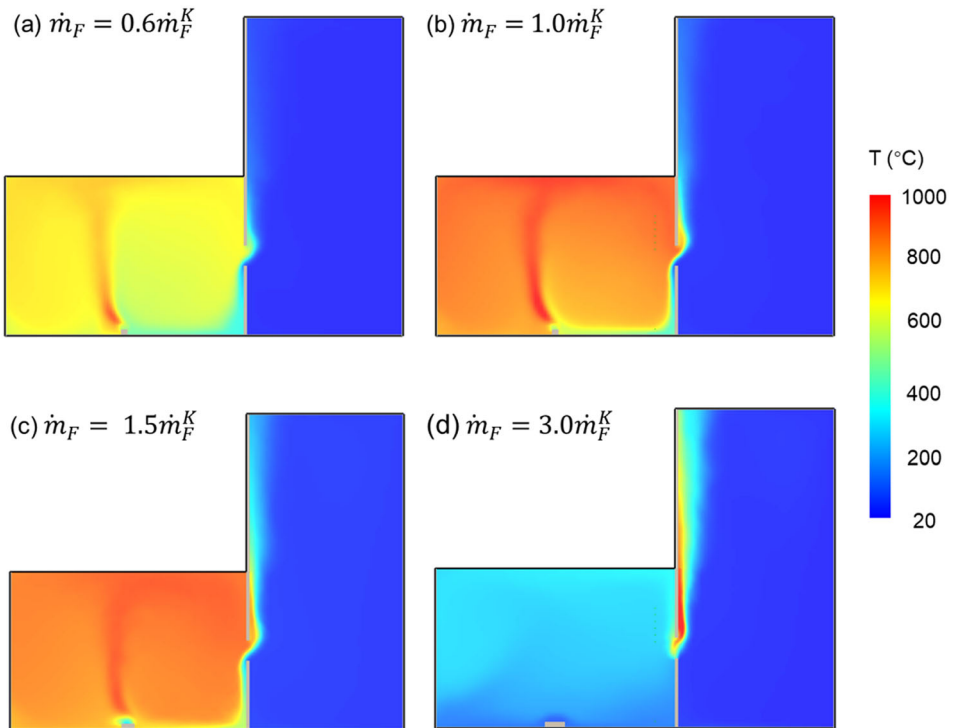


Figure 7. Time-averaged temperature distribution of the compartment fire with a 2.4 m by 0.3 m opening. ($A\sqrt{H} = 0.39$), under fuel generation rates of a 0.0069 kg/s ($0.6\dot{m}_F^K$ and 362 kW for an over-ventilated pre-flashover fire), b 0.0115 kg/s (\dot{m}_F^K and 603 kW at the flashover limit), c 0.0172 kg/s ($1.5\dot{m}_F^K$ and 904 kW for an under-ventilated post-flashover fire), and d 0.0345 kg/s ($3\dot{m}_F^K$ and 1.81 MW) jet flame.

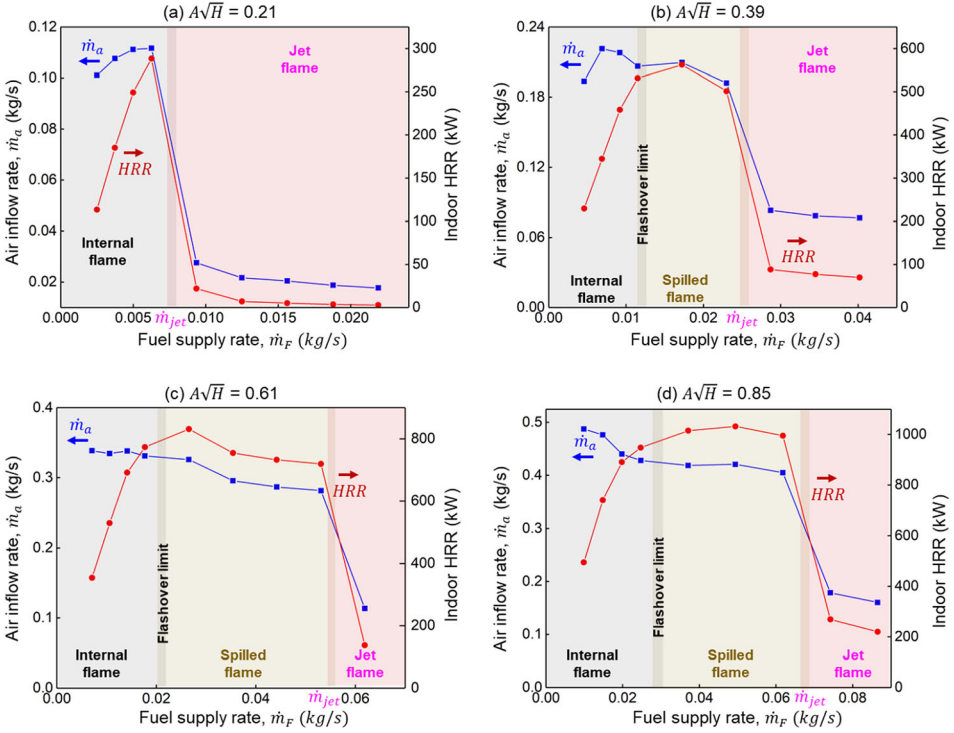


Figure 8. Air inflow rate (\dot{m}_a) and indoor HRR vs. fuel supply rates (\dot{m}_F) with ventilation factors ($AH^{1/2}$) of a $0.21 \text{ m}^{3/2}$, b $0.39 \text{ m}^{3/2}$, c $0.61 \text{ m}^{3/2}$, and d $0.85 \text{ m}^{3/2}$.

smoke and flame for a boundary layer near the wall due to the large aspect ratio and small critical fire HRR to generate spilled flame [34].

However, a special phenomenon occurs when the fuel supply rate reaches $3\dot{m}_F^K = 0.0345 \text{ kg/s}$, as shown in Figure 7d. Because the opening is quite small, the compartment is quickly filled with methane that injects out from the opening, just like the jet flame from a gas burner. At the same time, the air is unable to flow into the compartment to generate any HRR inside the compartment, so the temperature in the compartment is even lower than the over-ventilated pre-flashover fire in Figure 7a. The spilled jet flames only present near the opening and are attached to the wall, as they are pushed by the upward buoyancy force, which was also observed in early experiments by Thomas and Heselden [35].

Figure 8 further summarizes the evolution of (a) the inflow rate (\dot{m}_a) and (b) indoor HRR with an opening of a large aspect ratio (W/H). With the increasing fuel supply, the compartment fire behaviors with a short and wide opening show three stages, (1) the internal flame in the over-ventilated pre-flashover stage, (2) both internal and spilled flames in the under-ventilated post-flashover stage, and (3) a pure jet flame in the jet-flame stage, as shown in Figure 8b. For compartments with relatively a small ventilation factor (e.g., $A\sqrt{H} = 0.21$ in Figure 8a),

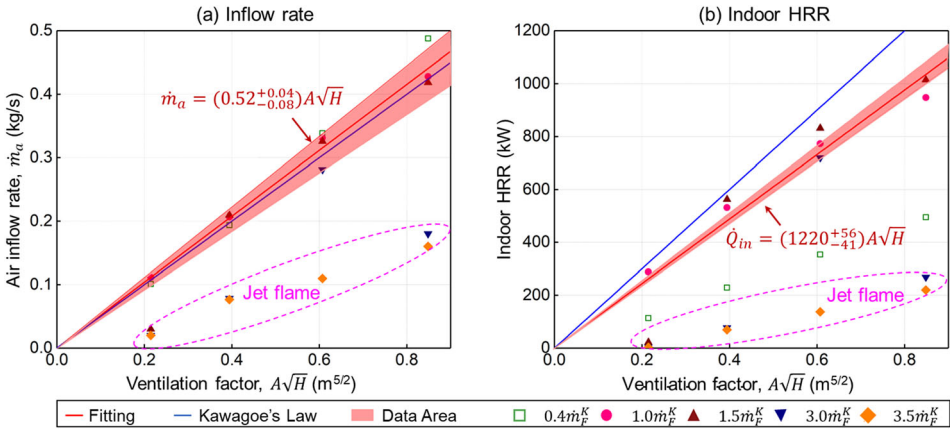


Figure 9. a Mass flow rate of inflow, and b indoor heat release rate under different fuel supply rates vs. ventilation factors in the 2-D model.

the compartment fire can even develop from the over-ventilated stage to the jet-flame stage directly. Similar fire behaviors had been observed in reduced-scale compartment fire experiments [33]. As the ventilation factor decreases, it becomes easier to form a jet flame under a lower fuel supply rate (\dot{m}_{jet}). When the jet flame is formed, the combustion in the compartment only exists near the opening, both the inflow rate (\dot{m}_a) and indoor HRR are drastically reduced. Especially, in fire scenarios with small ventilation factors, their HRR values are close to zero, so that Kawagoe’s Law is no longer applicable.

Figure 9 shows the air inflow rates (\dot{m}_a) and indoor HRR for the compartment fires in relation to the ventilation factors using the simplified 2-D model. Except for the jet flame stage, the average inflow rate ($\dot{m}_a = 0.52AH^{1/2}$) and indoor HRR ($\dot{Q}_{in} = 1220AH^{1/2}$) still follow the principle of Kawagoe’s Law. Table 3 further summarizes the inflow coefficient (C_a for all fire stages) and HRR coefficient (C_{HRR} for the under-ventilated post-flashover stage) and compares the literature data and 2D and 3D simulations in this study. Essentially, both the 2D and 3D numerical simulations can validate Kawagoe’s Law, and the uncertainty of the numerical simulations is within that of Kawagoe’s original experiments and other fire tests in the literature. When the compartment opening has a large aspect ratio, a special jet flame phenomenon can occur under a large fuel supply rate, i.e., beyond the limit of Kawagoe’s Law.

3.3. Compartment Fires with a Small Gap

The small gap, such as door gap or gap below eaves, is another special opening for a compartment, and many compartment fires are initiated in a largely confined room only with small gaps. For a leaky compartment with a small gap, the opening is too small to provide sufficient oxygen to sustain a big fire. Therefore, the smoke filling can be a significant process in the leaky compartment fire [36]. It is

Table 3
Comparison of Inflow Coefficient (C_a) in the form of $\dot{m}_a = C_a AH^{1/2}$ (kg/s) and indoor HRR coeicient (C_{HRR}) in the form of $\dot{Q}_{in} = C_{HRR} AH^{1/2}$ (kW), where all stages include both over-ventilated pre-flashover and under-ventilated post-flashover conditions

Source	Method	Scale	Fire stage	C_a	C_{HRR}
Kawagoe (1958) [5]	Experiment	Multi scales	All stages	0.50	–
Rockett (1976) [15]	Experiment	Full scale	All stages	0.40–0.61	–
Karlsson & Quintiere (1999) [1]	Theoretical	Multi scales	Under-ventilated	0.50	1518
Chow et al. (2005, 2012) [22, 23]	3-D simulation	Full scale	Over-ventilated	0.47/0.44	–
Lee et al. (2007) [8]	Experiment	Small scale	Under-ventilated	–	1500
Zhao et al. (2016) [24]	3-D simulation	Small scale	Under-ventilated	0.41	1131
Asimakopoulou et al. [25]	3-D simulation	Small scale	Under-ventilated	–	925
This work (Sect. 3.1)	3-D simulation	Full scale	All stages	0.44	1158
This work (Sect. 3.2)	2-D simulation	Full scale	All stages	0.52	1220

costly and challenging to study this dynamic filling process via large-scale fire experiments. For modeling the leaky compartment fire with CFD-based numerical simulation, it consumes a lot of computer resources, because the fire has a low indoor HRR, and the cell size should be even smaller than the small opening, and it is extremely time-consuming for a 3D model. To fully satisfy the two criteria mentioned in Sect. 2.3, a very fine mesh (~ 20 mm) is required to achieve an accurate prediction of the filling process. Therefore, the 2-D fire model with a very fine grid is applied, so that the total number of cells is still within acceptable limits, allowing fast and cost-effective modeling for leaky compartment fires.

Figure 10 shows a typical leaky compartment fire with a gap of 2.4 m by 0.1 m and a fuel supply rate of $\dot{m}_F^K = 0.029AH^{1/2} = 0.0022$ kg/s (see more details in

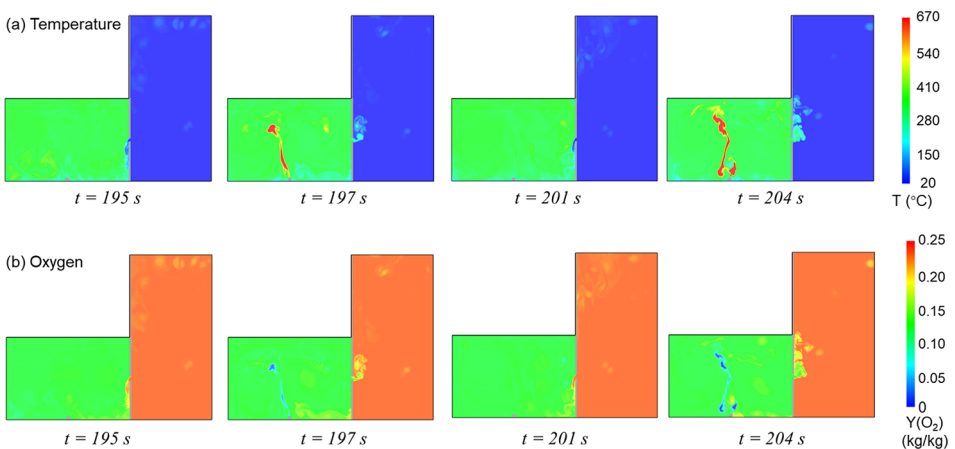


Figure 10. Numerical modeling of a the temperature distribution, and b the oxygen concentration vs. time for the leaky compartment fire (see more details in Video S3).

Video S3). In the early stages of fire development (e.g., with a smoldering fire or small flame), there is still much air in the compartment, which can maintain the initial fire growth. As the compartment temperature rises, the pressure in the compartment is higher than the ambient pressure, and the gases in the compartment begin to escape through the gaps to the outside, which prevents the inflow air (see 197 s in Figure 10b). Similar phenomena have also been recently observed in the air-tight compartment with mechanical ventilation [37, 38].

After the oxygen in the compartment is consumed, the combustion in the compartment is suppressed, and the cooling process will make the pressure in the compartment lower than the external ambient pressure. Thus, driven by the pressure difference, the fresh air can flow into the compartment through the small gap opening, which revitalizes the fire (see 204 s in Figure 10). The fire then increases the temperature and pressure inside the compartment and pushes hot gases out until the cooling process occurs again (i.e., repeating the process in Figure 10). This cycle with a period of about 7 s (or a frequency of 0.15 Hz) can be called a “deep-breathing” fire, which is different from the normal breathing observed in a compartment fire with large openings. In the deep-breath fire, the revitalization of fire occurs mainly in the vicinity of the fire source, and the continuous breathing processes are caused by the suppression of combustion due to insufficient oxygen (i.e., smothering). After about 300 s, with the continuous filling of unburned fuel and combustion products, eventually, the indoor fire and breathing process becomes interrupted and inhibited.

When the periodic deep-breath process occurs in the leaky compartment, the actual air inflow rate and indoor HRR change in a large range periodically, rather than reaching a steady value. Thus, Kawagoe’s Law can no longer predict the inflow rate and indoor fire HRR. As shown in Figure 11, the frequency of the deep-breath process remained nearly constant under different fuel supply rates and

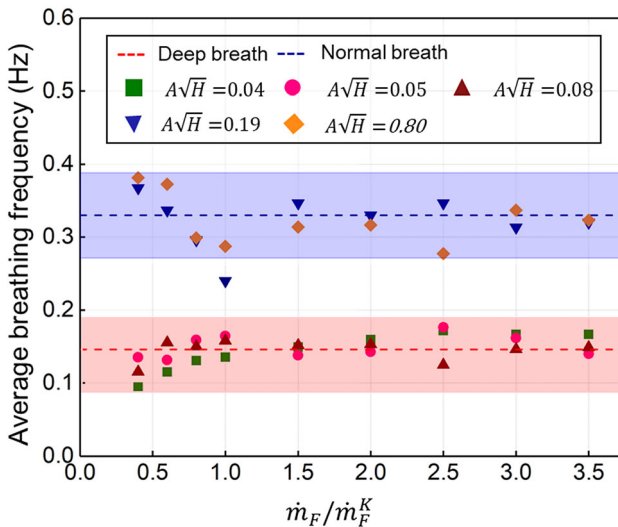


Figure 11. Average deep-breath frequency in a leaky compartment fire with different fuel supply rates and ventilation factors.

opening size from $AH^{1/2} = 0.04$ to 0.08 . Moreover, the frequency of a deep breath is much smaller than 0.33 Hz of normal breath found in the large openings ($AH^{1/2} \geq 0.19$), which is also a constant. Note that for the real fires in the leaky compartment, the frequency could be much longer and less regular due to the complex flaming and smoldering process of various solid fuels, which are not considered in the current numerical model. It is expected that the frequency of deep-breath fire will change with the size of the compartment (i.e., inertia) and fuel type so that further experimental and numerical explorations are needed in future work.

4. Conclusions

In the work, Kawagoe's Law is verified numerically for both over-ventilated and under-ventilated stages under different types of openings and predefined fuel supply rates. Both 2D and 3D numerical simulation results demonstrate that the Kawagoe's Law is applicable and accurate for fully developed compartment fires, with the air inflow rate ranging from $0.38AH^{1/2}$ to $0.56AH^{1/2}$ (kg/s). The indoor fire HRR changes from $1040AH^{1/2}$ to $1290AH^{1/2}$ (kW). Numerical results also show that both inflow rate and indoor HRR decrease with the increasing fuel supply rate, because of the preheating of inflow air and incomplete combustion under the reduced oxygen supply.

For compartment openings with a larger aspect ratio, the jet flame occurs more easily, and the fire inside the compartment will be suppressed completely under a large fuel supply rate, which cannot be described by Kawagoe's Law. Moreover, for leaky compartment fires with a small gap opening, due to the repeated revitalization and suppression of the fire, a low-frequency periodical deep-breath process can be observed numerically. This work numerically validates Kawagoe's Law and explores its limiting conditions, thus, providing practical guidance for modeling compartment fires and paving the way for constructing a numerical compartment fire database.

Acknowledgements

This work is funded by the Hong Kong Research Grants Council Theme-based Research Scheme (T22-505/19-N) and the PolyU Emerging Frontier Area (EFA) Scheme of RISUD (P0013879). TZ thanks the support from the Hong Kong PhD Fellowship Scheme.

Appendix A Summary of Kawagoe' pioneering work in 1950s

Report No. 27, "Fire Behavior in Rooms" [5] is a summary of Kawagoe's ten years of work from 1948 to 1958. In his report, different scales of compartment fire tests were conducted with compartment models and full-scale rooms, and the test list is summarized in Table A1.

Table A1
Kawagoe's compartment fire experiments in report No. 27, where fire duration is the time from the beginning of the room temperature rise to its maximum, and (× n) means n openings

Year	Test room (L × W × H, m)	Opening [#] (W × H, m)	Aspect ratio W/H [#]	AH ^{1/2} (m ^{2.5})	Fuel load (kg)	Fire duration (min)	m _F (kg/min)	m _F ^K (kg/min)
1948	0.40 × 0.40 × 0.20	0.32 × 0.1	3.2	0.01	0.32	6	0.053	0.055
1949–50	3.00 × 3.00 × 2.50	0.93 × 1.8	0.52	2.25	400	–	–	12.3
					400	23	17.4	
					890	60–70	13.7	
1950	1.00 × 1.00 × 1.00	0.3 × 0.6	0.5	0.14	20	24	0.83	0.77
		0.3 × 1.0	0.3	0.3	20	12	1.67	1.65
		0.3 (× 2) × 0.6	1.0	0.28	30	20	1.50	1.54
		0.39 × 1.0	0.39	0.39	20	10	2.00	2.15
		0.3 (× 2) × 1.0	0.6	0.6	30	9	3.33	3.3
1951	4.00 × 4.00 × 3.05	1.82 × 1.45 + 1.83 × 1.49	1.2	6.51	800	20	40.0	35.8
1951	2.53 × 1.85 × 1.45, 1.88 × 1.43 × 1.45	0.855 (× 2) × 0.75 + 0.425 × 0.5	2.28, 0.85	1.26	368	60	6.13	6.93
1952	3.80 × 2.40 × 2.58	1.80 × 1.36 + 0.90 × 1.36	1.32, 0.66	4.28	600	25–28	22.6	23.6
1952	4.30 × 3.48 × 2.47	1.65 (× 2) × 1.46	2.26	5.82	665	20–25	29.6	32.0
1953	4.00 × 3.60 × 2.80	2.00 × 1.00 + 2.00 × 1.16	2.00, 1.72	4.50	500	15–18	30.3	24.7
1953	3.60 × 3.60 × 2.50	0.65 (× 2) × 1.22 + 1.05 (× 2) × 1.22	1.06, 1.72	4.58	350	8–11	36.8	25.2
1955	4.20 × 4.20 × 3.87	2.8 (× 2) × 2.0	2.8	15.84	800	8–11	84.2	87.1
1956	5.20 × 5.20 × 5.30	0.98 (× 4) × 1.73	2.3	8.92	1250	20–25	55.6	49.0
1957	4.20 × 4.20 × 3.91	–	–	–	800	–	14	–

[#]The default number of opening is one. For multiple openings, the number is indicated by the bracket and “ + ”. The aspect ratio considers the total width of all openings

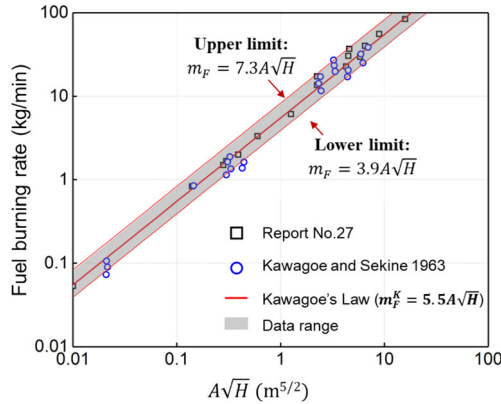


Figure 12. Comparison of fuel burning rate measured in Kawagoe’s early experiments and the uncertainty of the Kawagoe’s Law.

According to his experiment results, Kawagoe’s Law can be obtained using linear regression, which is consistent with his theoretical derivation [6]. All fuel burning rate data of Kawagoe’s pioneering experiment are replotted in Figure 12 to illustrate the accuracy and uncertainty of Kawagoe’s law in the form of Eq. (1), $\dot{m}_F^K = 5.5AH^{1/2}$ (kg/min). The upper and lower limits of the original test data are $\dot{m}_F = 7.3AH^{1/2}$ and $\dot{m}_F = 3.9AH^{1/2}$, respectively. Therefore, based on the experimental data, the uncertainty of applying Kawagoe’s law is about 30%.

Appendix B The temporal evolutions of temperature and air inflow rate

The temporal evolutions of temperature and air flow rate in the compartment fire with a 2.4 m (W) × 0.5 m (H) opening ($A\sqrt{H} = 0.85$) is taken as an example to clarify the semi-steady state from 600 to 1200 s. The ceiling temperature (TC1 and TC2) as well as the opening flow characteristics during the compartment fire can be seen in Figure 13, which shows that the fire has reached a semi-steady state between 600 and 1200 s.

Appendix C Impact of spilled flame on air inflow rate

The compartment with a 0.6 m (W) × 0.8 m (H) opening ($A\sqrt{H} = 0.43$) is taken as an example to show the impact of spilled flame on the air inflow rate. Compared with the over-ventilated fire scenario ($\dot{m}_F/\dot{m}_F^K = 0.8$), the air inflow rate under the under-ventilated fire scenario at the initial stage of the fire conforms to the description of Kawagoe’s Law. However, as the spilled flame heats the air outside the compartment, the air inflow rate begins to decrease and then reaches a semi-steady state (Figure 14).

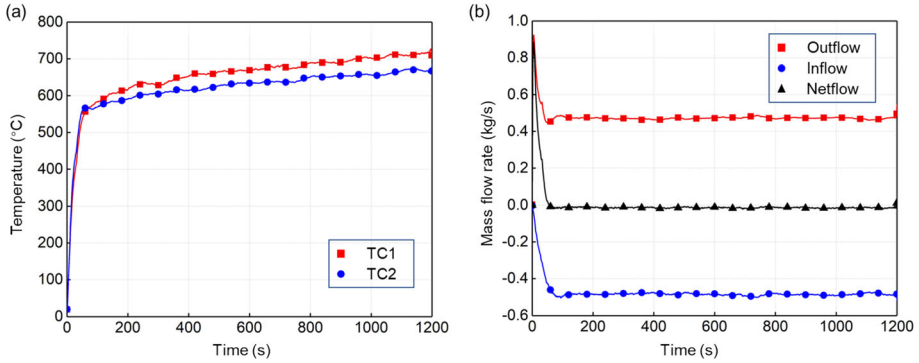


Figure 13. Temporal evolution of a temperatures at 0.1 m under the ceiling, b mass flow rate through the opening (2.4 m × 0.5 m and $A\sqrt{H} = 0.85$), where the HRR of the over-ventilated fire is 500 kW.

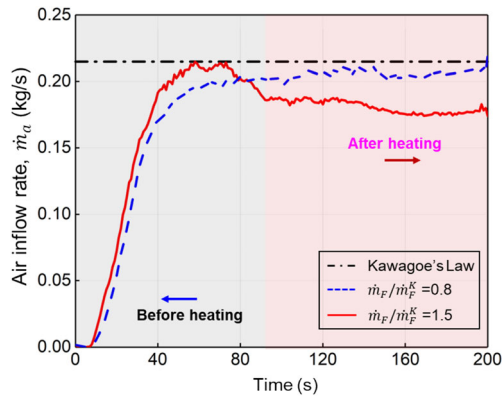


Figure 14. The temporal evolutions of air inflow rate with and without spilled flame under the compartment fire scenario with a 0.6 m (W) × 0.8 m (H) opening ($A\sqrt{H} = 0.43$).

SUPPLEMENTARY INFORMATION

The online version contains supplementary material available at <https://doi.org/10.1007/s10694-022-01218-1>.

References

1. Karlsson B, Quintiere J. Enclosure Fire Dynamics. 1999
2. McKenna ST, Jones N, Peck G, Dickens K, Pawelec W, Oradei S et al (2019) Fire behaviour of modern façade materials—understanding the Grenfell Tower fire. J Hazard Mater 368:115–123

3. Torero JL, Majdalani AH, Cecilia AE, Cowlard A (2014) Revisiting the compartment fire. *Fire Safety Science* 11:28–45
4. Thomas P (2004) SFPE classic paper review: Fire behavior in rooms by Kunio Kawagoe. *J Fire Protection Engin* 14:5–8
5. Kawagoe K (1958) *Fire Behavior in Rooms, Report 27. Tokyo, Japan*
6. Kawagoe K, Sekine T (1963) Estimation of fire temperature rise curves in concrete buildings and its application. *Bulletin of Japan Association for Fire Science and Engineering* 13:1–12
7. Huggett C (1980) Estimation of rate of heat release by means of oxygen consumption measurements. *Fire Mater* 4:61–65
8. Lee YP, Delichatsios MA, Silcock GWH (2007) Heat fluxes and flame heights in façades from fires in enclosures of varying geometry. *Proc Combust Inst* 31:2521–2528
9. Drysdale D. *An Introduction to Fire Dynamics*. 3rd ed. Chichester, UK: John Wiley & Sons, Ltd; 2011
10. Tang F, Hu LH, Wang Q, Lu KH, Yang LZ (2012) An experimental investigation on temperature profile of buoyant spill plume from under-ventilated compartment fires in a reduced pressure atmosphere at high altitude. *Int J Heat Mass Transf* 55:5642–5649
11. Pchelintzev VA. Study of the thermal system of fires in order to determine the limits of fire resistance required by structural elements. collected information on fire resistant building construction. *Central Research Institute for Fire Protection, Moscow* 1958
12. Simms DL, Wraight HG (1959) The temperature and duration of fires part ii-analysis of some full scale tests. *Fire Safety Science* 413:1
13. Simms DL, Hird D, Wraight HG (1960) The temperature and duration of fires: Part I: Some experiments with models with restricted ventilation. *Fire Safety Science* 412:1
14. Thomas PH (1960) Studies of fires in buildings using models. *Research* 13:87
15. Rockett JA (1976) Fire induced gas flow in an enclosure. *Combust Sci Technol* 12:165–175
16. Delichatsios MA, Silcock GWH, Liu X, Delichatsios M, Lee YP (2004) Mass pyrolysis rates and excess pyrolysate in fully developed enclosure fires. *Fire Saf J* 39:1–21
17. Johansson N, Svensson S (2019) Review of the Use of Fire Dynamics Theory in Fire Service Activities. *Fire Technol* 55:81–103
18. Thomas P, Heselden A, Law M (1967) Fully-developed Compartment Fires: Two Kinds of Behaviour. *Fire Research Station*
19. Fleischmann C, Parkes A (1997) Effects of ventilation on the compartment enhanced mass loss rate. *Fire Safety Science* 5:415–426
20. Asimakopoulou EK, Chotzoglou K, Kolaitis DI, Founti MA (2016) Characteristics of externally venting flames and their effect on the façade: a detailed experimental study. *Fire Technol* 52:2043–2069
21. Stavrakakis GM, Markatos NC (2009) Simulation of airflow in one- and two-room enclosures containing a fire source. *Int J Heat Mass Transf* 52:2690–2703
22. Chow WK, Zou GW (2005) Correlation equations on fire-induced air flow rates through doorway derived by large eddy simulation. *Build Environ* 40:897–906
23. Cai N, Chow WK (2012) Numerical studies on heat release rate in room fire on liquid fuel under different ventilation factors. *Int J Chem Engineering* 2012:9108
24. Zhao G, Beji T, Merci B (2016) Application of FDS to under-ventilated enclosure fires with external flaming. *Fire Technol* 52:2117–2142
25. Afflard A, Koutaiba EM, Asimakopoulou E, Kolaitis D, Zhang J, Lardet P (2019) Numerical Investigation of Fire Development in a Medium Scale Iso9705 Compartment-Façade Configuration. *Int. Symp. Fire Saf. Facades Paris, Fr. Sept. 26–27*

26. McGrattan K, Hostikka S, McDermott R, Floyd J, Weinschenk C, Overhold K. Sixth Edition Fire Dynamics Simulator User 's Guide (FDS). *NIST Special Publication 1019* 2020;Sixth Edit
27. Pikiokos D. Numerical simulation of compartment fires: investigation of opening flow characteristics 2016
28. Lock A, Bundy M, Johnsson EL, Hamins A, Ko GH, Hwang C, et al. NIST Technical Note 1603: Experimental study of the effects of fuel type , fuel distribution , and vent size on full-scale underventilated compartment fires in an ISO 9705 Room. 2008
29. McGrattan KB, Hostikka S, Floyd JE, McDermott R (2015) Fire Dynamics Simulator, Technical Reference Guide, Volume 3: Experimental Validation. *NIST Special Publication 1018 3*
30. Mowrer FW, Friday PA (2001) Comparison of FDS Model Predictions With FM/SNL Fire Test Data
31. McGrattan K, Floyd J, Forney G, Baum H, Hostikka S (2003) Improved radiation and combustion routines for a large eddy simulation fire model. *Fire Safety Science* 7:827–838
32. McGrattan KB, Baum HR, Rehm RG (1998) Large eddy simulations of smoke movement. *Fire Saf J* 30:161–178
33. Ren F, Hu L, Zhang X, Sun X, Zhang J, Delichatsios M (2019) Experimental study of transitional behavior of fully developed under-ventilated compartment fire and associated facade flame height evolution. *Combust Flame* 208:235–245
34. Ohmiya Y, Kang S, Noaki M, Delichatsios MA (2020) Effects of opening aspect ratio on facade gas temperatures with and without sidewalls for underventilated conditions. *Fire Safety J* 113:102944
35. Thomas PH, Heselden AJM (1962) Behaviour of fully developed fire in an enclosure. *Combust Flame* 6:133–135
36. Quintiere JG. Principles of fire behavior, Second Edition. 2016
37. Li J, Beji T, Brohez S, Merci B (2021) Experimental and numerical study of pool fire dynamics in an air-tight compartment focusing on pressure variation. *Fire Saf J* 120:103128
38. Li J, Beji T, Brohez S, Merci B (2020) CFD study of fire-induced pressure variation in a mechanically-ventilated air-tight compartment. *Fire Saf J* 115:1030